Mercury: The Image of the Planet in the 210°–285° W Longitude Range Obtained by the Short-Exposure Method

L. V. Ksanfomality

Space Research Institute, Russian Academy of Sciences, Profsoyuznaya ul. 84/32, Moscow, 117810 Russia
Received April 29, 2003

Abstract—For the purpose of obtaining images of the unknown portion of Mercury, we continued the previously started series of observations of this planet by the short exposure method. Several thousand electronic images of Mercury have been acquired on 1–2 May 2002 under good meteorological conditions at the high-altitude Skinakas Astrophysical Observatory of Iraklion University (Crete, Greece, 35°13′ E, 24°54′ N) during the evening elongation. The phase angle of Mercury was 95°–99° and the observed range of longitudes was 210°–285° W. Observations were carried out using Ritchy–Chrétien telescope (D = 1.29 m, F = 9.857 m) with the KS 19 filter cutting wavelengths shorter than about 700 nm. The planet's disk was seen, on average, at an angle of 7.75″ arcsec. The image scale was equal to 47.8 μm/arcsec. We used a CCD with a pixel size of 7.4 × 7.4 μm in the regime of short exposures. By processing a great number of electronic images, we succeeded in obtaining a sufficiently distinct synthesized image of the unknown portion of Mercury's surface. The most prominent formation in this region is a giant basin (or cratered "mare") centered at about 8° N, 280° W, which was given a working name "Skinakas basin" (after the name of the observatory where observations were made). By its size, the interior part of this basin exceeds the largest lunar Mare Imbrium. As opposed to Mare Imbrium, the Skinakas basin is presumably of impact origin. Its relief resembles that of Caloris Planitia but the size is much larger. A series of smaller formations are also seen on synthesized images. The resolution obtained on the surface of Mercury is about 100 km, which is close to the telescope diffraction limit. Also considered are the published theoretical estimations of the possible advantages offered by the short exposure method. Some results obtained by other research groups are discussed.

INTRODUCTION

The first and as yet unique mission to Mercury, *Mariner 10,* was carried out in 1973–1975. The apparatus was placed on a planetary orbit and approached the planet periodically. Resources of the orbiter's systems were exhausted after the third approach to Mercury. In all three approaches to the planet in 1973–1975, the orbiter was over the same sunlit hemisphere of the planet. *Mariner 10* images covered about 35% of the planet's area (Vilas *et al.*, 1988). Although some researchers argue that the images covered nearly 50% of the area, this statement is based on obvious misunderstanding: the mosaic imaging was carried out from distances 300 to 700 km, which, with regard to the planet's diameter of 4880 km, restricted the coverage by no more than 35% of the surface. Processing of the images of edge zones allowed the coverage to be increased to 46% (Grard and Balogh, 2001). Almost the entire imaged surface is similar topographically to "highland" regions of the Moon (Fig. 1); there are no lunar-type maria (lava regions) on this side of the planet. Increased interest of researchers in the relief of the unknown portion of Mercury is explained, in particular, by the fact that the new planned planetary missions, Messenger and BepiColombo, need for a large body of original data, including information on the surface of Mercury, especially for choosing the landing

site of the BepiColombo probe (called the Surface Element, Battrick, 2000; Grard and Balogh, 2001). Unfortunately, the Hubble space telescope cannot be used to take Mercury's images because there is great risk, in view of the small angular distance between Mercury and the Sun, of damaging the telescope equipment by direct solar light. For the same reason, the administration of observatories is reluctant to afford opportunities of using large telescopes for observations of Mercury. However, as will be shown below, such images can yet be obtained by ground-based technical and analytical means at the limit of technical possibilities. The short exposure method was found to be of the most promise for obtaining Mercury's images (Ksanfomality, 2002).

THEORETICAL ESTIMATION OF THE POSSIBILITIES OF THE SHORT EXPOSURE METHOD

In recent years, considerable progress has been achieved in obtaining resolved images of Mercury using electronic images obtained with short exposures by ground-based technique. For this purpose, CCDs and sophisticated programs for computer processing of initial data are normally used. The idea of using short exposures has long been known, and several attempts to theoretically estimate a possible gain in resolution have been reported. Fried (1978) pointed out that "there is a
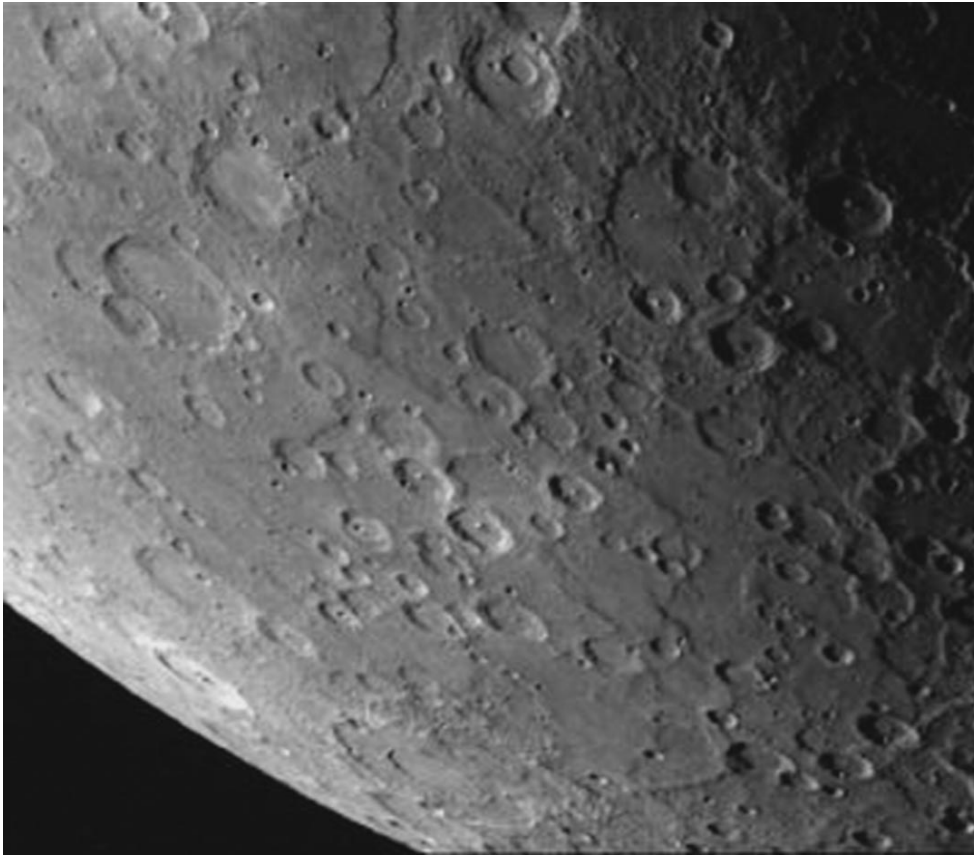
Fig. 1. The structure of a portion of Mercury's surface imaged by *Mariner 10* (fragment) is similar to continental regions of the Moon. The impact crater sizes on Mercury, at the same scales of impact events, are about half as large as those on the Moon because of greater free fall acceleration.

probability of achieving a nearly diffraction-limit resolution in taking images of an object observed through a turbulent medium because of a negligible instant distortion of the wave front on the aperture." However, the short exposure method remained unrealized for a long time because of low sensitivity of photographic materials. Only with the advent of CCD matrices with high quantum yield, taking, in particular, resolved (albeit on a limited scale) electronic images of Mercury became possible.

The then available experimental data showed that a decrease of exposure does really improve significantly the resolution of astronomical images. If we assume that the short exposure method allows an approach to the diffraction limit, it is easy to evaluate a limiting potential gain in resolution. The typical resolution for moderate-sized telescopes (with the diameter D of about 1.2 m) generally constitutes $1.0'–1.5'$, which is, at the wavelength $\lambda = 550$ nm, 9 to 13 times poorer resolution than the diffraction limit equal to $1.22\ \lambda/D$. The real (low) resolution is determined mainly by atmospheric turbulence. According to the author's observations, the characteristic time during which the instant optical properties may change rarely occurs to be shorter than 30 ms. This time depends on observation

site, day time, density of the aerosol constituent of the atmosphere, and, of course, on zenith distance of an object (the air mass sec z). The short exposure method differs fundamentally from the known adaptive optics technique in that it makes use of instantaneous overcast breaks in the atmosphere. An exposure reduction does not eliminate distortions caused by irregularities in air lenses but decreases substantially image blurring. Having accumulated a significant number of electronic images, one can then select low-distortion images suitable for subsequent processing.

For Mercury, observing conditions are additionally complicated by a large air mass (sec z) due to great zenith distances z of the planet and by a high brightness of morning or evening sky in the periods of the planet's visibility. Finally, the conditions of visibility of the planet are such that its effective observations are possible only at high-altitude observatories located at southern latitudes.

Considering the major characteristics of the short exposure method, Fried (1978) makes reference to a short paper by Hufnagel (1966), where the author pointed out that the probability of obtaining a "good" image (with resolution close to the diffraction limit)

changes as a negative exponential function of the square of aperture diameter. The paper by Fried was first reported at the scientific conference "Propagation of Optical Radiation through the Atmosphere", which was held under the aegis of NATO, and its initial title was "How many images are necessary in order to obtain one good image?" Fried (1978) made a detailed analysis of wave-front distortions by atmospheric turbulences. Distortions impairing resolution of astronomical instruments are introduced by atmospheric density inhomogeneities with characteristic size r and extent along the ray r_o. The parameter r_o is defined as the diameter of the coherent zone constrained by turbulence. According to D. Fried, for an instrument with diameter greater than $3.5r_o$, the turbulence-constrained resolution is λ/r_o and the possible gain in resolution may reach 3.4 at short exposures. Fried gives the following expression for the "probability of a lucky short exposure" p:

$$p \approx 5.6\exp[-0.1557(D/r_o)^2]. \qquad (1)$$

It may be concluded that as the telescope diameter increases, the situation becomes nearly hopeless. Because observations of Mercury are always limited in time, they have to be occasionally performed under windy weather. In his calculations, Fried gives a useful assessment of the role of the constant component of wind velocity perpendicular to the line of sighting. In this case, the adopted criterion—the changes in the inclination of the wave front—do not exceed $1/2 \, (\lambda/D)$ if the exposure length t is

$$t = r_o/2V. \qquad (2)$$

As a consequence, it is indicated that observations before dawn, when atmospheric turbulence is still absent, are most favorable, whereas in daytime observations (with small zenith distances) rather long exposures can be obtained at weak daytime winds. Fried (1978) noted, in conclusion: "It is important to remember that turbulence statistics and the quantity r_o were assumed to be constant during experiment. What was calculated is the probability that the image selected from the ensemble of distorted wave fronts will have insignificant distortions."

Mendillo *et al.* (2001) also analyze the conclusions drawn by Fried (1978) in his study. These authors consider some relationships and summarize the main inferences as follows. "At a fixed turbulence scale r_o, the probability p sharply drops with increasing the telescope diameter D. For $D/r_o = 5$, one "good" image falls on ten short exposure images and for $D/r_o = 10$, one of the million images turns out to be quite good." As will be shown below, the conclusions drawn by Fried (1978) and Mendillo *et al.* (2001) about the advantages offered by small (~0.5 m) telescopes seem to be disputable and raise serious doubts because they do not apparently take into account a number of circumstances, for example, the fact that an exposure with 1.5-m telescope may
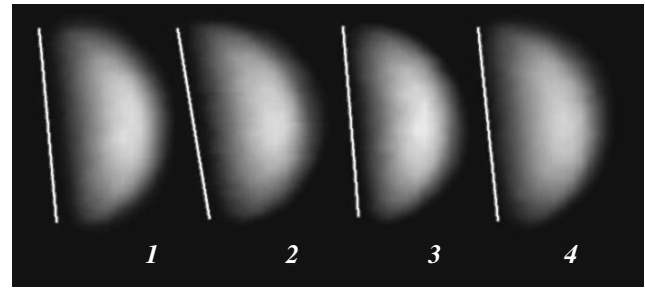

Fig. 2. Rotation of successive images in the plane of the sky. Exposures are 1 ms each.

be one order of magnitude shorter than with 0.5 m telescope, at the given signal-to-noise ratio. Moreover, the number of photons per one pixel received by a high-resolution CCD is always limited and susceptible to significant fluctuations. A good result can therefore be obtained only by combined processing of many hundreds and even thousands of electronic images. At the same time, an accessible time of observations of Mercury is, as known, so limited that the required amount of experimental material can be obtained only with sufficiently large instrument, when the net exposure time constitutes a small portion of the total observational time. Our observations of Mercury have been carried out on three instruments (at different times) with diameters of optics 0.406, 1.25 and 1.30 m. No doubt, the latter diameters proved to be the best.

As for any theoretical study, the conclusions drawn by Fried (1978) are valid only within the premises adopted. Along with the aforementioned factor (the exposure length), there are probably other unaccounted factors as well. For example, small rotations of successive images in the plane of the sky are observed in series of observations with considerable number of electronic images (see the fragment of observations on May 2, 2002, shown in Fig. 2). Here, white lines drawn in parallel to the terminator demonstrate dramatically this strange effect. We failed to explain it by differential refraction because images *1–4* are slightly spaced in time. It is not clear what atmospheric phenomena are responsible for the image rotation—the little-known but real fact, which hampers the processing of experimental data.

As regards the experimental data concerning a relatively long-period evolution and decay of atmospheric instabilities, Ksanfomality *et al.* (2002) showed, using the short exposure method, that they arise during a few seconds or tens of seconds, the fact that further restricts the possibilities of small instruments. However, no less interesting are faster variations shown in Fig. 3, where a fragment is presented of the sequence of frames (also taken from May 2, 2002 observations) obtained with an exposure of 1 ms at 99-ms intervals. Diffuse images *1* and *3* differ greatly from a distinct image *2*. In the orig-
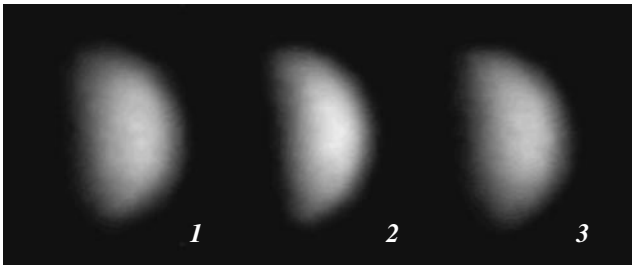
Fig. 3. Fast changes in image quality. Image *2* is distinct; images 21 and *3* are diffuse. Intervals between successive images *1–2* and *2–3* are 99 ms. Exposures are 1 ms.

inal materials, tens of images to the left of image *1* and to the right of image *3* are also indistinct.

OBSERVATIONS OF MERCURY DURING APRIL–MAY 2002 ELONGATION

After the first, relatively successful results obtained in 1999 at the Abastumany Astrophysical Observatory, the next series of observations of Mercury was carried out only in 2001. Observations were made at the same observatory on November 1–8, 2001, during the period of morning visibility of the planet, using an up-to-date STV CCD. We employed the AZT-11 telescope (with $D = 1.25$ m and the Cassegrain focus $F = 16$ m) with a filter cutting wavelengths shorter than 700 nm. Despite the small CCD pixel size (7.4 × 7.4 μm for the STV CCD), the long-focus instrument has advantages for observing Mercury, since it provides the nominal resolution. At the same time, owing to the high object brightness, the time of acquisition in each pixel of several thousands of signal units required for further processing is still no greater than a few milliseconds. The processing of observation results (Ksanfomality, 2002) made it possible to obtain images, the quality of which was much superior to that achieved in the preceding study (Ksanfomality *et al.*, 2001). Nevertheless, the processing showed that the body of information contained in about 50 "good" electronic images is still inadequate for obtaining convincing images of the unknown portion of the planet.

The problem associated with a shortage of information was overcome by observing Mercury during its evening elongation in April–May 2002 at the Skinakas observatory of Iraklion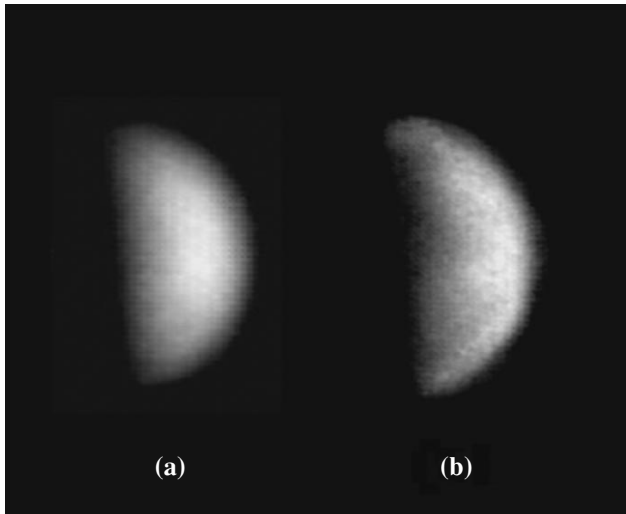 University (Crete, Greece). The obvious advantage of this observatory for observations of Mercury is its position (24°54′ N, 35°13′ E) at low latitude. We employed the STV CCD with a 7.4 × 7.4 μm pixels. On 1–2 May 2002 we succeeded in obtaining several thousand of electronic images of the planet under good meteorological conditions. Observations were carried out on the Ritchy–Chrétien telescope with $D = 1.29$ m and $F = 9.857$ m, equipped with the glassy filters KS 17 and KS 19 cutting wavelengths shorter than 670 and 700 nm, respectively. The long wavelength boundary was determined by the spectral properties of the CCD, which have been described earlier in (Ksanfomality *et al.*, 2001) together with other relevant information about the STV CCD. The planet's disk was seen on May 1–2, on average, at an angle of 7.75″ and had a linear size of 0.556 mm in the telescope focal plane. On the CCD, this size corresponds to 50 lines in the high-resolution ("zoom") mode. The phase angle of Mercury was 95°–99°.

As opposed to the observations made in 2001, the maximum zenith distance z was limited by the telescope automatics and was less than 72°; as a result, there was a significant bright sky background even with cutting filters employed. The reflecting coating of the main mirror had a great number of defects, which caused an additional light scattering and consequently rendered polarimetric measurements impossible.

We used short exposures, mostly 1 ms, and up to 10 ms at extremely large z. Small image size allowed application of a "grab" program for rapidly collecting and entering images into the flash memory with a period of 100 ms, which allowed a great number of original images to be obtained. An example of a single image out of 336 that were taken in one of the groups in the zoom mode is shown in Fig. 4a. The image was not processed; however, large relief features, such as a large dark region near the terminator, north of the equator, can be clearly distinguished. Nevertheless, obtaining high-quality images requires no less than several hundred original electronic images. After preliminary rejection, about one-half of the images generally remained. Further selection, which was performed with the aid of a special program or by hand, inevitably contained the operator's errors, which were then revealed by the program. For example, only 23 of 70 "very good," manually selected images entered into the synthesized image for preliminary processing (Fig. 4b). Defects of this image are evident. For this reason, further processing used a database containing a few thousand images.

Observations of Mercury on May 1–2, 2002

Date	Mercury's phase	Subterral diameter	Visible diameter	Geocentric distance	Heliocentric distance	Stellar magnitude
1.05.2002 16:30 UT	95°.5	283°	7.7″	0.89	0.35	+0.1
2.05.2002 16:40 UT	99°.4	286°	7.8″	0.87	0.36	+0.2

first was obtained in the range 16:15–16:19 UT and the second, in the range 16:53–16:55 UT.

Fig. 4. (a) Initial unprocessed electronic image of Mercury. (b) Preliminary processing of a group consisting of 23 initial images.

It should be noted that the proof of reality of image features remains a constant problem in the synthesis of images of the unknown part of Mercury. While for longitudes covered by *Mariner 10* imaging (i.e., for meridional segments 120°–190° W and 0°–50° W) the reality of features can be confirmed by comparing images with a photomap, in all other cases only the recurrence of features for independently collected material may be considered as a proof of their reality. Since the surface of Mercury is completely unknown in the 210°–285° W longitude range, the only criterion of reality of surface features was their presence in several independently obtained synthesized images.

In the present study the results of processing of two image series performed on May 2, 2003, are given. The

IMAGE PROCESSING AND VERIFICATION OF REALITY OF THE RESULTS OBTAINED

The process of obtaining and processing of images included the following eight steps.

1. Taking images by the short exposure method. 2. The standard "flat field" correction. 3. The choice of a series of undistorted or single images. 4. Correlative alignment. 5. The choice of the level for the "unsharp mask" operation. 6. Lucey–Richardson's or de Sitter's deconvolution procedure. 7. Image correction by eliminating the darkening to the limb and terminator. 8. Plotting the longitude/latitude grid.

The selection of undistorted images and their correlative alignment were the most important and labor-intensive procedures. Next, the optimal depth of "unsharp mask" was chosen for selecting fine details. The image resolution can be improved using Lucey-Richardson's or de Sitter's deconvolution procedure, which, however, distorts the linearity of the brightness scall. As a whole, we used for processing a package consisting of 16 programs, among which the main were a new AIMAP 225 program developed by Kakhiani in 2002 and the programs Astrostack and Astrostack2 (Stekelenburg, 1999, 2002). This is essentially an improved program package, which has already been used for processing observations in 2001 (Ksanfomality *et al.*, 2001).

The probable synthesis error is most convenient to assess using as an example the processing of observations made in 2001 (at latitudes from 90° to 190°), because, on the one hand, the original data were very limited at that time and, on the other, the results could be compared to the photomosaics of *Mariner 10* images. The best image constructed on the basis of the
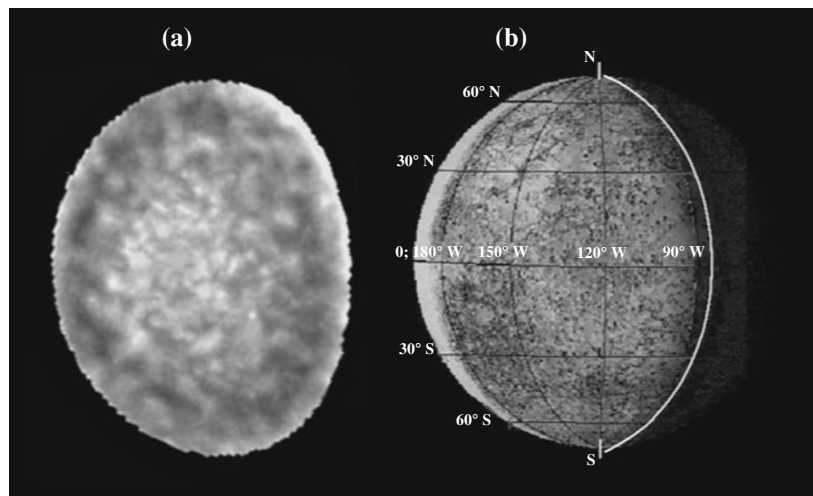
Fig. 5. (a) Image of Mercury synthesized from November 3, 2001, observations and (b) the photomap composed of the image mosaics obtained by *Mariner 10*.
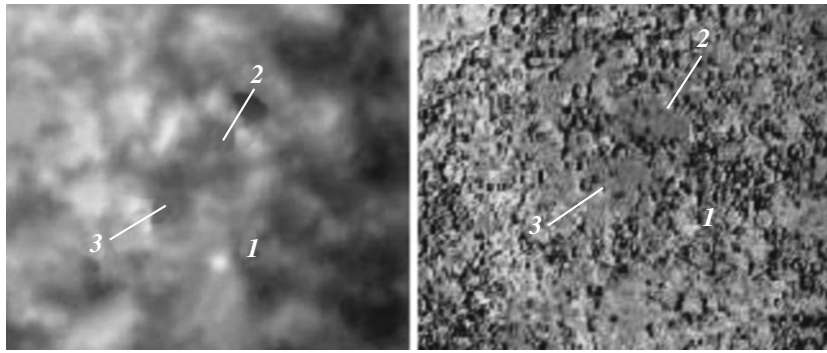
Fig. 6. Comparison of a fragment of a synthesized image (left) with the photomap of Mercury (right).

Section passing through dot *1* in Figs. 5 and 6 parallel to polar axis
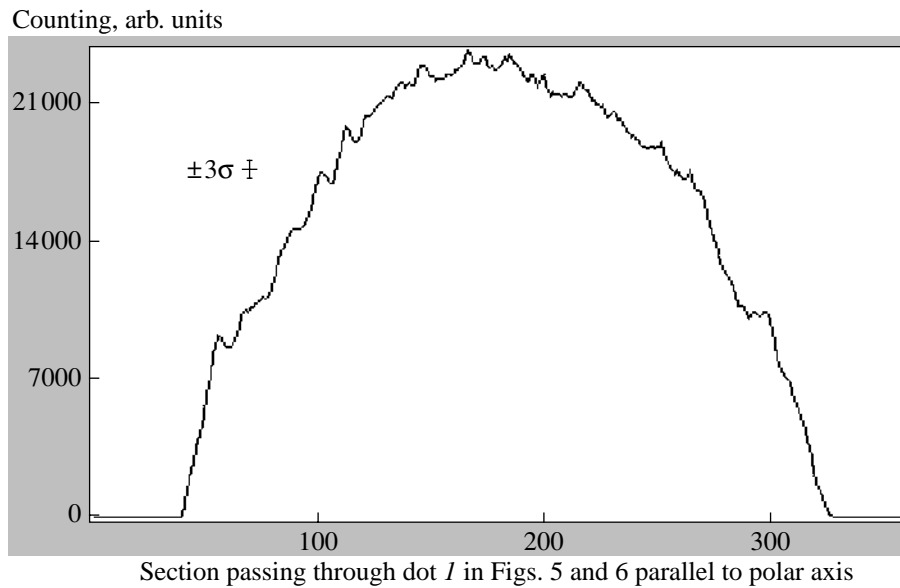
Fig. 7. Contrasts along the vertical section in Fig. 5a.

2001 data is shown in Fig. 5, where fine details are well outlined but large dark and bright areas are nearly absent. As was established later, low spatial frequencies were suppressed during processing because of insufficient original data and poor filtration provided by the unsharp mask operation. The results of identifying randomly selected features reported earlier in (Ksanfomality, 2002) are shown in Figs. 5a and 5b. An example of coincident features in two image fragments is illustrated in Fig. 6. A minor bright dot 1 (10° S, 117° W) in Fig. 5a coincides with an unnamed bright crater in Phaethontias Regio (Fig. 6). Two large dark rounded regions *2* and *3* near the equator (centered on 5° N, 124° W and 1° S, 135° W) have the same form in Fig. 6b. These regions include the craters Mena (0.5° N, 125° W) and Lysippus (1.5° N, 133° W). The features in other areas were also identified. Some details in Fig. 5a may be of noise origin in view of the limited number of original images. Nevertheless, the similarity of both images in Fig. 6 is obvious despite small size of

formations presented here (feature *3* is only 200 km in width).

Ultimately, the features of synthesized images of Mercury represent contrast elements that he within the range 4–10% in Fig. 5a. Figure 7 shows the distribution of contrast features in the section parallel to the polar axis and passing through the bright dot *1* in Figs. 5 and 6. The position of features across the section is marked on the linear scale. It is not difficult to estimate the root-mean-square (r.m.s) error for a signal obtained from one pixel of the CCD. For example, the number n of processed images in Fig. 5a was 42, the mean signal value R was 1293, and the sum of squares of absolute errors $\Sigma \Delta R_i^2$ was 131721. The r.m.s error and the relative r.m.s error are, respectively,

$$\sigma_R = \sqrt{\Sigma \Delta R_i^2 / n(n-1)} = 8.75 \quad \text{and} \quad \sigma_R/R = 0.68\%. \tag{3}$$
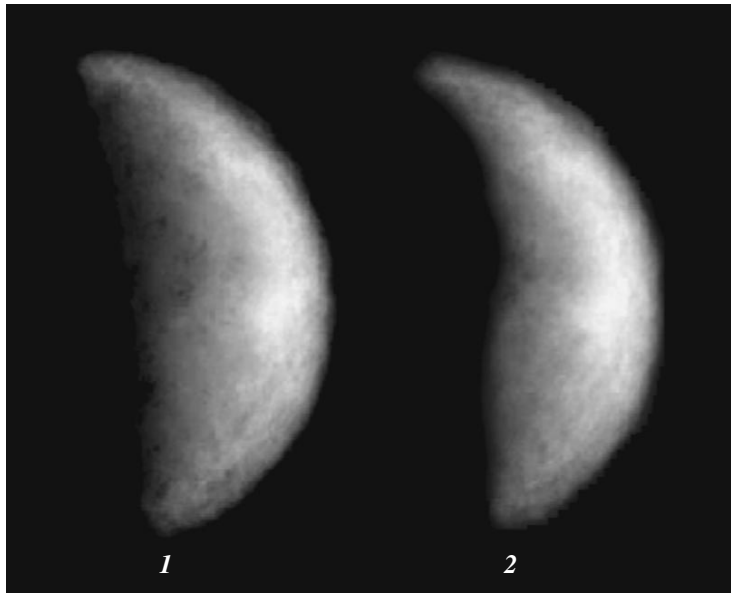
Fig. 8. Images *1* and *2* synthesized from two independent files of the original data obtained on May 5, 2002.

Therefore, the threefold error bar $3\sigma_R \approx 2\%$ is comparable, in principle, to the image contrast on individual pixels. However, the image of features is formed by not a single element but a large group of elements (1200 pixels in Fig. 6), the erroneous combination of which is considerably less probable. The program of image processing specifically isolated contrast transitions, whereas low-contrast extended features were suppressed because of insufficient information to reconstruct them.

The conditions for synthesis of Mercury's images based on observations of the planet during the April–May 2002 elongation were much better in view of an ample material obtained. Figure 8 shows two images synthesized from two independent original groups of electronic images taken on May 2, 2002: image *1* is obtained using the group corresponding to the time interval 16:15–16:19 UT and image *2* is synthesized from the group of original pictures corresponding to the interval 16:53–16:55 UT. Distinctions are observed only in fine details of images and in the depth of their contrast. The number of original images in group 1 was 560 and in group 2, about 900. The preliminary selection, as was said above, was made by hand; we eliminated images with significant geometric distortions, defocused images and those having technical defects caused by imperfect computer programs used in observations.

Correlative alignment made it possible to obtain the image presented in Fig. 9a.

MERCURY'S SURFACE IN THE LONGITUDE RANGE 210°–285° W

Synthesized image of Mercury, together with a superimposed coordinate grid, is shown in Fig. 9b. Identification of coordinates is only tentative, but the error is hardly larger than several degrees because we indicate only the centers of albedo and relief features. The description of albedo and relief features revealed in the image is also to be considered as tentative.

The most prominent large formation in the longitude range between 210 and 285° W is a large basin (or a crater "mare") that lies on the terminator and centered at about 8° N, 280° W. The working name of this formation—the Skinakas basin—is chosen after the name of the observatory where observations were made. The available material does not permit a unique treatment of the dark portion of the annular depression surface as a cratered "mare" or as a region filled with mafic lava rocks; therefore, it would possibly be well to use a standard term "plain" used in the Mercurian nomenclature. However, we used here a more common term "basin" as applied in identifying vast annular depressions on the surfaces of planets and satellites.

The Skinakas basin has a double rim with diameter 25° (1060 km) of the interior part and twice as large diameter of a distinguishable outer rim. By its size, the interior portion of this basin slightly exceeds the largest lunar Mare Imbrium, while the outer part has the size of the lunar Oceanus Procellarum. Taking into account the properties of the Skinakas basin, the widespread opinion that Mercury's relief is mainly of highland nature (by the lunar terminology) should be referred only to
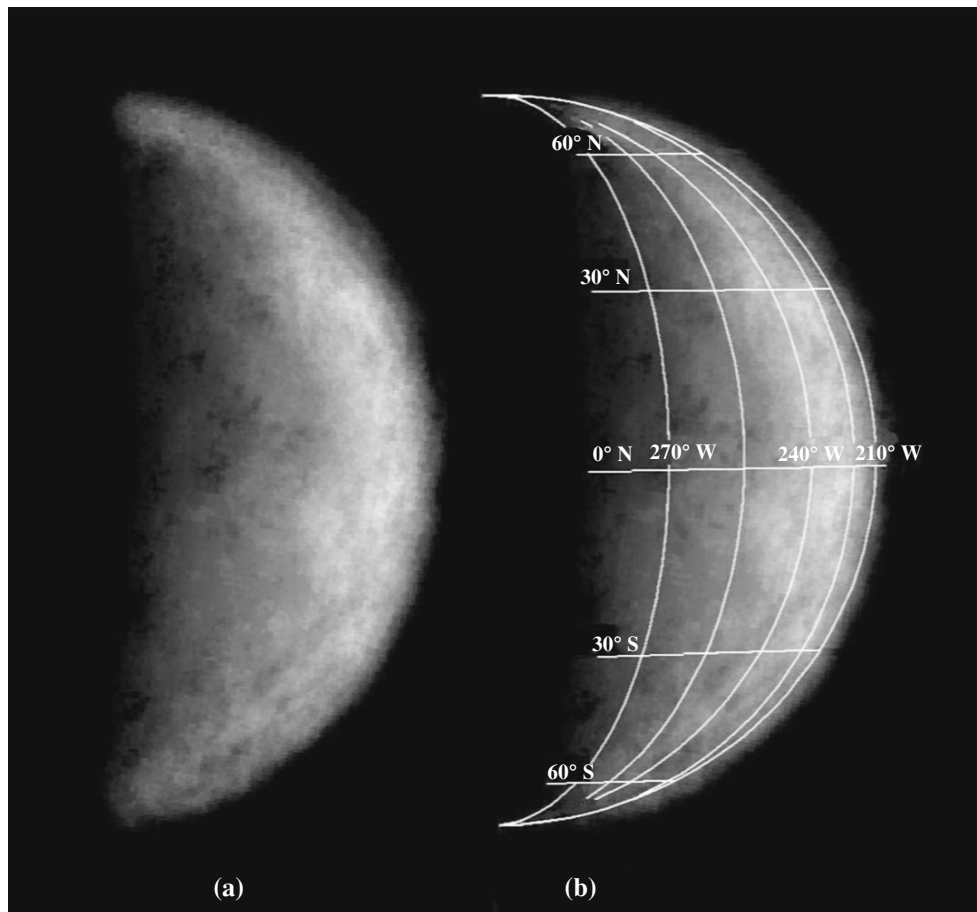
Fig. 9. Image of Mercury in the 210°–285° W longitude range synthesized using the results of observations of Mercury in April–May 2002. The same image with superimposed coordinate grid is shown on the right.

the *Mariner 10* imaged portion of the planet, which, however, includes an extensive cratered plain Caloris Planitia. Unlike Mare Imbrium, the Skinakas basin has, according to Fig. 9a, a central hill of impact origin, whereas the surface of Mare Imbrium represents a lava field, which was formed in the ancient epoch of global lava eruptions on the Moon. At least, the size of the Skinakas basin also points to a very large (and probably early) impact phenomenon.

A few somewhat smaller formations are traced on both independent original synthesized images. A dark field of about 250 km in size on the terminator (Fig. 9) is located in the high-latitude region (at about 65° N, 270° W). Two large bright regions, each about 1000 km wide in the latitudinal direction, are located near the limb, with their centers at 25° N, 225° W and 10° S, 250° W, respectively. A dark long (2000 km) strip (probably, a valley?) located near the southern horn of Mercury extends from 20° S, 230° W to 55° S, 275° W and goes away beyond the terminator. An area with complex topography is seen near 60° S, 245° W. A dark field is located on the terminator at 45° S, 285° W. In the previously published radar images (Harmon *et al.*,

2001) large craters are present in polar zones, but we failed to identify them with the formations shown in Fig. 9 because of inadequate resolution.

The limiting achieved resolution in Fig. 9 approximately corresponds to the diffraction resolution of the instrument, which is equal to about 100 km on Mercury's surface; it coincides with the resolution achieved earlier in (Ksanfomality, 2002; Ksanfomality *et al.*, 2002).

COMPARISON WITH OTHER EXPERIMENTAL RESULTS OBTAINED IN 1995–2001

The results described below were obtained by processing observations of Mercury carried out by various researchers. The revised processing of these data (Ksanfomality *et al.*, 2001) allowed the image shown in Fig. 10 to be obtained. On the left side of this image we show the first results obtained at the Abastumany Astrophysical Observatory on December 3, 1999, during the morning elongation. Observations were tentative and carried out using a primitive low-resolution CCD with an exposure of 10 ms (Ksanfomality *et al.*, 2001). Nev-
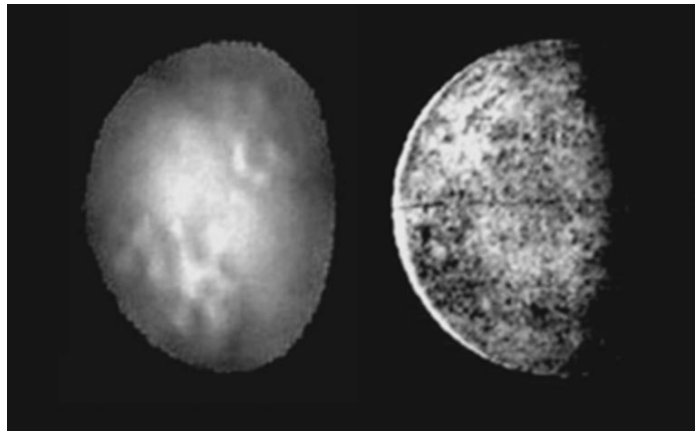
Fig. 10. The synthesized image of Mercury obtained from the December 3, 1999 data (left); the photomap composed of *Mariner 10* image mosaics (right). Subterral meridian is 120° W, the phase angle is 76°.

ertheless, the processing of these observations not only demonstrated small differences in albedo of large areas on Mercury (Fig. 10), but it also confirmed the promise of the short exposure method. Comparison to the *Mariner 10* photomap demonstrates significant differences explained by the composite character of this photomap (where phase effects were eliminated) and by the insufficient experimental material included in the processing procedure. The mosaic character of the photomap also makes the identification with the photomap more difficult because different portions of the map were taken at different phase angles. The limb darkening on the photomap (on the right part of Fig. 10) is absent. The author has no more reliable experimental data for these longitudes and Mercury's phase. Because of the differences in longitudes, a comparison to the new results is useless.

One of the pioneering investigations of Mercury, in which ground-based CCD observations were made by the short exposure method, has been carried out by Warell at the Astronomical Observatory at Uppsala, Sweden, and by Limaye at University of Wisconsin–Madison, USA. Warrell started his investigation in 1995 (Warell and Lymaye, 2001) using a CCD installed at the focus of the 0.5-m solar telescope and exposures between 25 and 360 ms. In his papers, he published single (not averaged) images (Fig. 11), which are naturally inferior to those obtained by processing of large data files.
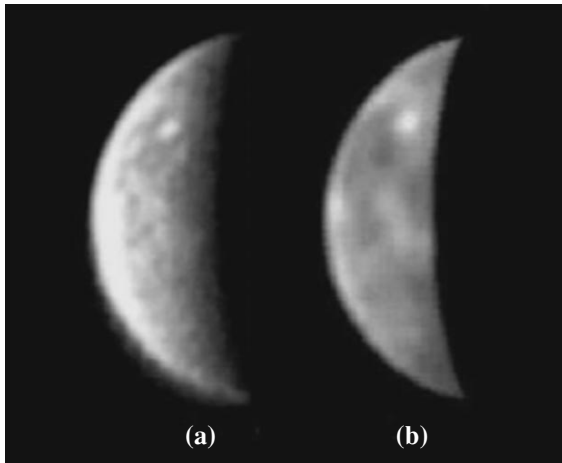
On August 29, 1998, Dantowitz *et al.* (2000) obtained an image of one of the regions of Mercury, which had not been covered by *Mariner 10* imaging in 1974. Observations were carried out by the short exposure method in good meteorological conditions on the Mount Wilson Observatory 60 inch (1.5 m) reflecting telescope using a CCD mounted at the Cassegrain focus. The imaging was conducted for 10 min at a speed of 60 frames per second with an exposure of 16.7 ms. A video image was registered in an analog mode. The resulting images were combined and pro-

cessed by the unsharp mask method. The image of Mercury presented by Dantowitz *et al.* (2000) and shown in Fig. 12a was constructed by processing 40 selected electronic images. The subterrestrial point corresponds to 7.7° N, 254° W. In the image, we can distinguish the areas widely different in albedo. The brightest object in the upper part of the image (at 35° N, 300° W) is likely to be a young impact crater. The phase angle of Mercury in the image is 106°.

At the same day and on the same telescope, observations of Mercury were performed by another research group (Baumgardner *et al.*, 2000). They used a standard video camera installed at the 1.5 m telescope. Imaging was made in a digital mode with the same frame fre-
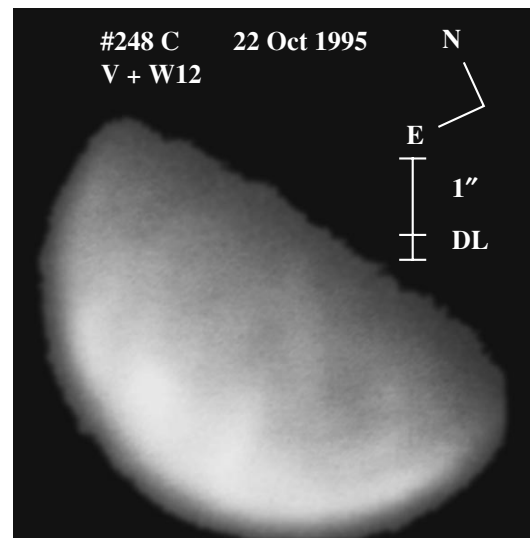
Fig. 11. Image of Mercury obtained during the October 1995 elongation. A fragment of the figure is taken from (Warell and Limaye, 2001). Orientation of the planet and the 1″ scale are shown in the image. The DL bar indicates the telescope diffraction limit.

Fig. 12. Processing of observations of Mercury at the Mount Wilson observatory on August 29, 1998: (a) Data from (Dantowitz *et al.*, 2000), (b) data from (Baumgardner *et al.*, 2000).

quency and exposure. The total number of frames in a video clip taken on August 29, 1999, was 219 000, and 1000 frames were selected for further processing. The best image of Mercury taken from (Baumgardner *et al.*, 2000) is shown in Fig. 12b). Albedo features are clearly seen but undoubted signatures of hand-made processing cause justifiable concern: such a regular and contrast boundary cannot be present on the terminator (the normal appearance of Mercury's terminator is seen on the left-hand side of the image in Fig. 12). It is likely that the authors eliminated phase effects and artificially straightened the terminator. In a paper by Mendillo *et al.* (2001, Figs. 11 and 12b), comparison is made of the results obtained by these authors. They find a similarity in the images obtained and claim that a 250-km resolution on the surface of Mercury was achieved in their study. Comparison of the data obtained by Dantowitz *et al.*, 2000) and Baumgardner *et al.*, 2000) with our new results is also impossible because of the differences in longitudes.

The results of processing observations obtained on November 3, 2001, at the morning elongation of Mercury at the Abastumany Astrophysical Observatory have already been considered above (Figs. 5, 6 and 7). Comparison with new results is also impossible because of the differences in longitudes.

CONCLUSIONS

New observations of Mercury have been carried out at the evening elongation by the short exposure method on May 1–2, 2002, at the Skinakas Astrophysical Observatory of Iraklion University (Crete, Greece, 35°13′ E, 24°54′ N). Under favorable meteorological conditions, a few thousand electronic images of the planet have been obtained. Observations were con-

ducted with a Ritchy–Chrétien telescope ($D = 1.29$ m, $F = 9.857$ m) with the KS 19 filter cutting wavelengths shorter than 700 nm. An STV-type CCD with $7.4 \times 7.4\ \mu m$ pixels was employed. The planet's disk was seen, on average, at an angle of 7.75″. The angle of Mercury's phase was 95°–99°. Short exposures, mainly 1 ms, were used in observations.

Observations encompassed the surface of Mercury in a range of longitude between 210° and 285° W. Here, a large cratered "mare" centered at roughly 8° N, 270° W has been found. The basin has a double rim with a diameter of the interior part of about 25° (1060 km) and twice as large diameter of the outer rim. By the size of the inner rim, this formation exceeds Mare Imbrium on the Moon. The relief of the crater basin is apparently similar to that of Caloris Planitia.

Despite the difficulties in observations of Mercury and the limited duration of possible observations, we were able to obtain, under good atmospheric conditions, original electronic images suitable for synthesis of resolved images of the planet. Further work will possibly permit the observers to obtain at the nearest years, using ground-based facilities, maps of the whole surface of the planet at resolution close to the diffraction limit.

REFERENCES

Battrick, B., BepiColombo Interdisciplinary Mission to Planet Mercury, European Space Agency, 2000.

Baumgardner, J., Mendillo, M., and Wilson, J.K., Digital High-Definition Imaging System for Spectral Studies of Extended Planetary Atmospheres. 1. Initial Results in White Light Showing Features on the Hemisphere of Mercury Unimaged by *Mariner 10, Astron. J.*, 2000, vol. 119, pp. 2458–2464.

Dantowitz, R.F., Teare, S.W., and Kozubal, M.J., Ground-based High-Resolution Imaging of Mercury, *Astron. J.*, 2000, vol. 119, pp. 2455–2457.

Fried, D.L., Probability of Getting a Lucky Short-Exposure Image through Turbulence, *J. Opt. Soc. Am.*, 1978, vol. 68, no. 12, pp. 1651–1658.

Grard, R. and Balogh, A., Returns to Mercury: Science and Mission Objectives, *Planet. Space Sci.*, 2001, vol. 49, pp. 1395–1407.

Harmon, J.K., Perillat, P.J., and Slade, M.A., High-Resolution Radar Imaging of Mercury's North Pole, *Icarus,*, 2001, vol. 149, pp. 1–15.

Hufnagel, R.E., Restoration of Atmospherically Degraded Images, *Proc. Nat. Acad. Sci.*, 1966, vol. 3, Append. 2, p. 11.

Ksanfomality, L.V., Dzhapiashvili, V.P., Kakhiani, V.O., *et al.*, Experiment on Obtaining Mercury's Images by the Short Exposure Method, *Astron. Vestn.*, 2001, vol. 35, no. 3, pp. 208–213 [*Sol. Syst. Res.* (Engl. transl.), 2001, vol. 35, no. 3, pp. 190–194].

Ksanfomality, L.V., High-Resolution Imaging of Mercury Using Earth- based Facilities, *Astron. Vestn.*, 2002, vol. 36, no. 4, pp. 291–301 [*Sol. Syst. Res.* (Engl. transl.), 2002, vol. 36, no. 4, pp. 267–277].

Ksanfomality, L.V., Dzhapiashvili, V.P., Kakhiani, V.O., *et al.*, Evaluation of the Possibilities of the STV CCD Detector for the Observations of Planets, *Astron. Vestn.*, 2002, vol. 36, no. 4, pp. 366–373 [*Solar Syst. Res.*, (Engl. transl.), 2002, vol. 36, no. 4, pp. 341–347].

Mendillo, M., Warell, J., Limaye, S.S., *et al.*, Imaging the Surface of Mercury Using Ground-based Telescopes, *Planet. Space Sci.*, 2001, vol. 49, pp. 1501–1505.

Stekelenburg, R., AstroStack Manual (v. 0.90 beta). 1999. http://www. Astrostack. Com/

Vilas, F., Surface Composition of Mercury from Reflectance Spectrophotometry, in *Mercury*, Vilas, F., Chapman, C.R., and Matthews, M.S., Eds., Tucson: Univ. of Asrizona Press, 1988, pp. 59–76.

Warell, J. and Limaye, S.S., Properties of the Hermean Regolith: I. Global Albedo Variation at 200 km Scale from Multicolor CCD Imaging, *Planet. Space Sci.*, 2001, vol. 49, pp. 1531–1552.